Entry into the Stockholm Junior Water Prize 2012

Modeling and Environmental Analysis of Hydraulic Fracturing in Upstate New York

Kunal Sangani, New York

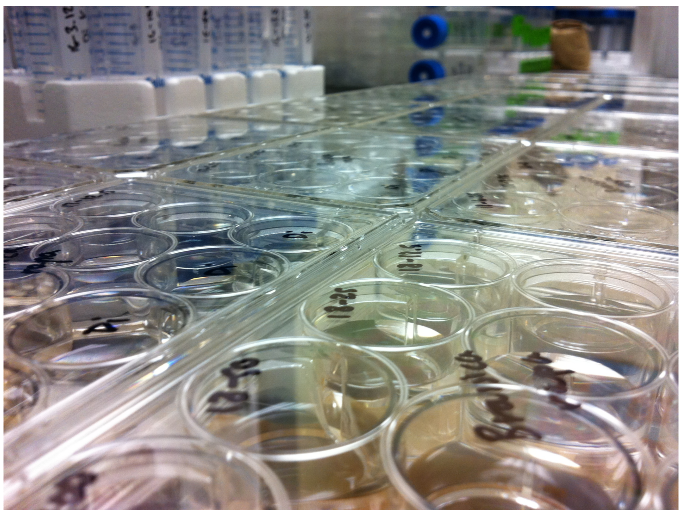

Abstract

This study provides a comprehensive examination of the various aspects of hydraulic fracturing in Upstate New York. A model was developed to determine the effect of process parameters on gas production; predictions of the model were shown to match public data from Marcellus Shale wells. The model demonstrated that utilizing fracturing pressures of 40-50 MPa could produce an equivalent amount of natural gas over a 30 year period while mitigating damage to rock structures. An average well produces 1.0-3.5 million gallons of highly contaminated brine called flowback water. Chemical analysis showed that effluents have high concentrations of barium, strontium, and lead, and exhibit beta decay, most likely attributed to Pb^{210} isotopes. These measurements are perhaps the first documentation of metal ion concentrations and radioactivity in hydraulic fracturing effluent. An 'established ecosystem' experiment showed that heavy metals may accumulate in *B. rapa* plant tissues, thus allowing for biomagnification. Finally, effluent was found extremely toxic to freshwater organisms such as *Hydra oligactis*; EC_{50} values and LC_{50} values were as low as 3.7% and 11.1%, respectively.

Table of Contents

Biography and Acknowledgements:

My name is Kunal Sangani, and I am a senior at Fayetteville-Manlius High School in Syracuse, NY. In my free time, I enjoy playing on my school's tennis team, playing piano, skiing, and attending Model United Nations competitions as a part of my school's MUN club. Next year, I will be attending Stanford University for Computer Science. This is my second water-related research project in high school; previously, I worked with Mishka Gidwani, currently a freshman at Cornell University, on devising a new method for oil spill remediation using a naturally-produced phytoplankton exopolymer. For my research, I have previously been named a Siemens Competition Regional Finalist and an Intel STS Semifinalist. I have also attended Intel ISEF twice, winning First Place in the Environmental Management Category last year. The breadth of this research project required that I work across several different labs-- in the course of completing this project, I worked across three universities and five labs, as well as devising numerical modeling methods at home and conferring with experts in the field across the nation. Because of this, I owe much of my research to people that helped me along the way: Dr. Miriam Rafailovich, Ms. Rebecca Grella, Ms. Lourdes Collazo, Dr. Cindy Lee, Mr. David Hirschberg (Stony Brook University), Dr. Neal Abrams, Ms. Deb Driscoll (SUNY ESF), Dr. Eric M. Lui, Dr. Don Siegele (Syracuse University), Mr. Craig Barnes (Rochester Kodak Facility), and Dr. Mark Zoback (Stanford University).

Introduction:

According to the Potential Gas Agency's 2011 estimate, the United States possesses 1,898 trillion cubic feet of natural gas, worth more than eight trillion dollars at current prices (Curtis, 2011). Until recently, scientists believed that the large quantities of natural gas stored in shales, approximately 36% of these total reserves, could not be accessed safely and efficiently. Rogner (1997) noted that large quantities of natural gas are known to exist in Devonian shales, but "only minor efforts have been made to delineate them." The appearance of new technologies, particularly horizontal drilling and hydraulic fracturing, has made retrieval of these fuels possible (Karlsson et. al., 1992). Hydraulic fracturing, commonly called 'hydrofracking,' involves the injection of fracturing fluids at high pressures to overcome principal stress forces and create apparent tension in rock structures (Ameen, 1995). Substantial fracturing increases the permeability of shale rock and allows for the mobility of stored natural gas. Paired with horizontal drilling techniques, a single well on average is able to collect 2.8 billion cubic feet (bcf) of gas over a thirty year lifetime (Considine, 2010).

This study is primarily concerned with the Marcellus Shale (Figure 1), which has recently gained attention as a large and previously-untapped source of fuel extending from Upstate New York through Pennsylvania to West Virginia (Harper, 2008). The Marcellus Shale is expected to be developed over 95,000 square miles, with a gas content of 363-500 trillion cubic feet of gas (Soeder, 1986). Development of the formation is also predicted to create upwards of 200,000 jobs in the northeast.

Figure 1. The Marcellus Shale Extends from Upstate New York to West Virginia. Picture from http://oilshalegas.com/sitebuildercontent/sitebuilderpictures/mar.JPG

However, several environmentalists have voiced concerns on potential ramifications of hydraulic fracturing. Opposition to the process is largely centered on the ability of methane and fracturing fluid toxins to migrate through rock toward shallow water aquifers, and the treatment of large quantities of flowback and produced waters. Osborn et. al. (2011) found a correlation between methane concentrations in private drinking water wells and their proximity to hydraulic fracturing sites; no evidence, however, was found linking radon or heavy metal levels to nearby gas wells. Concern was also raised over the release of more than 15 million gallons of untreated hydrofracture effluent from Pennsylvania' Josephine facility to Blacklick creek (Volz et. al., 2011).

There is a relative dearth of literature that has been published on hydraulic fracturing; much of the process's details, including the exact composition of fracturing fluids injected into shale formations, are preserved as trade secrets. Additionally, without sufficient data on the irregularities of shales several thousands of feet underground, it is difficult to predict the geological effects of hydraulic fracturing.

Thus, this study has three aims: (1) to create a numerical model of hydraulic fracturing in the geological context of the Marcellus Shale in Upstate New York; (2) to analyze the chemical composition of Marcellus Shale effluent; and (3) to assess the toxicity of hydrofracture effluent to plants and aquatic organisms in Upstate New York ecosystems. Modeling of the hydraulic fracturing process will be presented first, followed by laboratory experimentation and results.

Modeling:

This study was primarily interested in creating a model within the geologic context of Upstate New York. A version of the stratigraphic column provided by Hill and Lombardi (2002) is shown in Figure 2. The Marcellus Shale is found approximately 1450 m below the earth's surface, and has a thickness of 60 m. The material properties of each rock layer are given by Karacan et. al. (2006). Any simplified model must (1) account for the changes in rock permeability caused by hydraulic fracturing and (2) be able to predict the amount of natural gas that can be collected over a period of time. Changes in permeability depend on the stress produced by high-pressured fluids in the borehole; therefore, a detailed stress analysis is necessary.

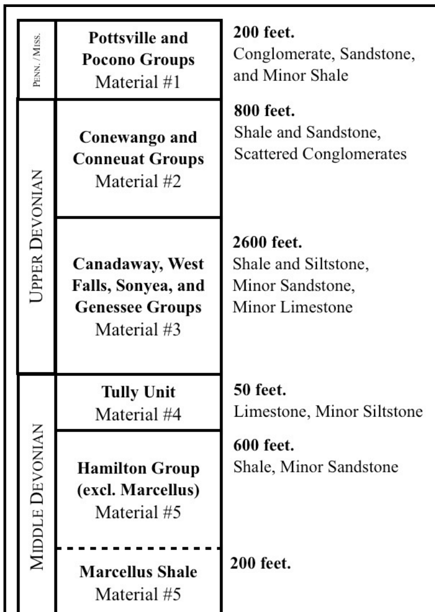

Figure 2. Stratigraphic Rock Column of Upstate New York. The Marcellus Shale is given at a depth of ~1450 m. Adapted from Hill & Lombardi (2002).

Since the flow occurs primarily near the wellbore, stress analysis was required in its vicinity. For this purpose, the simplified model shown in Figure 3 was used. The region considered around the wellbore was given a radius (r_o) of 30 m, corresponding to half the height of the Marcellus Shale in Upstate New York. Since the depth at which hydraulic fracturing occurs is much greater than this radius, it can be assumed that differences in the hydrostatic pressure through the height of the area are negligible. Therefore, the outer circular boundary exerts a pressure (P_o) of 35 MPa, equal to the hydrostatic pressure of the rock matrix shown in Figure 2. The applied wellbore pressure, P_i, produces both a radial and angular stress distribution. In particular, the angular stress distribution for an elastic medium is given by Lamé's Equation:

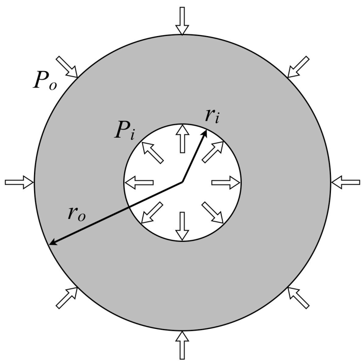

Figure 3. Geometry for Stress and Flow Analysis near a Wellbore. The above thick-walled cylinder is representative of the Marcellus Shale.

$$\sigma_\theta(r) = \frac{r_i^2 P_i - r_o^2 P_o}{r_o^2 - r_i^2} + \frac{(P_i - P_o) r_i^2 r_o^2}{(r_o^2 - r_i^2) r^2} \tag{1}$$

where r_i is the radius of the wellbore. A positive value for σ_θ would imply a tensile stress, desirable for fracturing rocks. This condition is satisfied when $P_i(r_i^2 + r_o^2) > 2P_o r_o^2$. Since r_i is typically much smaller than r_o, this condition can be simplified to $P_i \geq 2P_o$. Given a hydrostatic pressure P_o of 35 MPa, a wellbore pressure of 70 MPa would be required to create tensile stress for fracturing. Current pressures used in the field vary between 60-100 MPa.

At a depth of 1500 m, the high compressive stress due to hydrostatic pressure closes most pores, and the permeability of the rock is greatly reduced. Fractures created by the tensile stresses, however, can significantly increase the permeability of the rock. An empirical correlation, relating the permeability to the change in stress, is given by Karacan et. al. (2006):

$$k = Ke^{0.25(\sigma - \sigma_o)} \tag{2}$$

where K is the original permeability of the rock, σ (in MPa) is the stress in the rock (in this case, given by σ_θ), and σ_o (in MPa) is the original stress in the rock. Shale rock is anisotropic, meaning that its permeability is different in the horizontal and vertical directions. Karacan et. al. (2006) give K equal to 1.0×10^{-16} and 2.0×10^{-16} m^2, for the vertical and horizontal directions, respectively. For the purpose of this study, the permeability was assumed to be isotropic, with $K = 1.5 \times 10^{-16}$ m^2.

The above relations form the foundation for a modeling of natural gas flow. Flow is approximated by Darcy's equation $u = -(k/\mu)\partial P/\partial r$, where u is the velocity, k is the permeability of the rock matrix, μ is the viscosity, and P is the pore pressure. Immediately after the fluid pressure on the wellbore is released, the inside of the wellbore is close to atmospheric pressure. Note that the hydrostatic pressure is relatively unchanged, and is supported by the rock matrix and proppant material that was injected during the fracturing process. The pore pressure near the wellbore is close to atmospheric pressure (0.1 MPa), but far from the wellbore it remains close to 35 MPa. This difference in pore pressure drives the flow of natural gas toward the wellbore.

To determine how the pore pressure near the wellbore varies over time, I used a mass balance for a radial element (Figure 4). The masses of gas entering and leaving the element in time *dt* are given by:

$$\text{mass in} = \rho r \frac{k}{\mu}\frac{\partial P}{\partial r}\bigg|_{r+dr} L d\theta dt \text{ ; mass out} = \rho r \frac{k}{\mu}\frac{\partial P}{\partial r}\bigg|_{r} L d\theta dt \quad (3)$$

where ρ is the density of the gas and *L* is the horizontal length of the well. During time *dt,* the pore pressure inside the element is also changing. The change in the mass of gas inside the pore is given by:

$$\text{mass change} = \varepsilon r \left(\frac{\partial \rho}{\partial P}\right) L dP dr d\theta \quad (4)$$

where ε is the porosity of the rock. The conservation of mass therefore gives:

$$\frac{\partial}{\partial r}\left(\rho \frac{\partial P}{\partial r}\frac{k}{\mu} r\right) = \varepsilon \left(\frac{\partial \rho}{\partial P}\right) r \frac{\partial P}{\partial t} \quad (5)$$

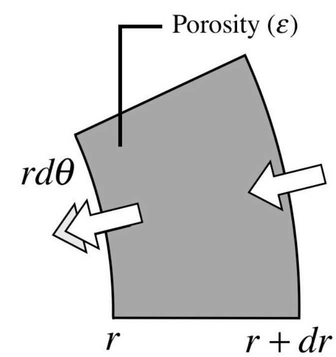

Figure 4. A Single Radial Element in the Flow Model. This element provides the basis for the mass balance. It is assumed that the element's pores are occupied by natural gas.

The left-hand side of (5) accounts for the mass of gas entering and exiting the element by Darcy's Law, and the right-hand side accounts for the mass of the gas released due to the change in pore pressure. (5) simplifies to the following non-linear parabolic partial differential equation (Farlow, 1993) for *P*:

$$\frac{\partial P}{\partial t} = \frac{1}{\varepsilon r}\frac{\partial}{\partial r}\left(P \frac{\partial P}{\partial r}\frac{k}{\mu} r\right) \quad (6)$$

The above equation was solved subject to boundary conditions: $P = P_{atm}$ (0.1 MPa) at $r = r_i$ and $\partial P/\partial r = 0$ at $r = r_o$. The latter boundary condition assumes that there is no natural gas present beyond a radial distance of r_o. The initial condition was: $P = P_o$ for all values of $r > r_i$.

A computer program was written in MATLAB to solve the above problem numerically using the finite differences method (Smith, 1986). Equation (6) was first rearranged for this purpose as:

$$\frac{\partial P}{\partial t} = f\frac{\partial^2 P}{\partial r^2} + \frac{1}{r}\frac{\partial}{\partial r}(rf)\frac{\partial P}{\partial r} \text{ where } f = f(r,t) = \frac{k(r)}{\varepsilon\mu}P(r,t) \quad (7)$$

The r domain was divided into N logarithmically-equidistant divisions, with $\log r_{j+1} - \log r_j = (\log r_o - \log r_i)/N$, $j = 1,2,\ldots N$. Next, the derivatives of P were approximated using implicit central difference formulae:

$$\frac{\partial P}{\partial r}(r_j, t) = \frac{P(r_{j+1}, t+\Delta t) - P(r_{j-1}, t+\Delta t)}{(r_{j+1} - r_{j-1})} \tag{8}$$

$$\frac{\partial^2 P}{\partial r^2} = \frac{2[h_L P(r_{j+1}, t+\Delta t) + h_R P(r_{j-1}, t+\Delta t) - (h_R + h_L)P(r_j, t+\Delta t)]}{h_R h_L (h_R + h_L)^2} \tag{9}$$

where $h_R = r_{j+1} - r_j$ and $h_L = r_j - r_{j-1}$. The function f and its derivative were evaluated based on the distribution of P at time t, and permeability k was evaluated using Equations (1) and (2). The boundary condition at $r = r_o$ was satisfied by requiring that $P(r_N) = P(r_{N+1})$. This process resulted in a set of (N + 1) linear equations for $P(r_j, t+\Delta t)$, $j = 1,2,\ldots N+1$, which were solved using MATLAB. The time step Δt was initially given as 0.002 months, and subsequent values were chosen to be inversely proportional to the maximum change in P at any r.

Figure 5a shows the distribution of P for selected values of time t (in months). These calculations were carried out with P_o = 35 MPa, P_i = 70 MPa, r_o = 30 m, r_i = 0.1 m, N = 200, ε = 0.10, and $\mu = 2.0 \times 10^{-5}$ Pa·s. At this fracturing pressure, the permeability k at r_i was equal to 9.5×10^{-13} m^2, almost four orders of magnitude larger than the initial permeability (1.5×10^{-16} m^2). As a result, the pressure changes rapidly near the wellbore, and has a nearly constant value at larger distances. This constant pressure decreases with time, as the gas from the reservoir depletes.

Figure 5b shows the total gas production from the well as a function of time for various fracturing pressures. To determine production, the volumetric gas flow was evaluated using:

$$Q(t) = \int_0^t \frac{2\pi r_i k L}{\mu} \left.\frac{\partial P}{\partial r}\right|_{r=r_i} dt \tag{10}$$

where horizontal length of the well (L) was taken to equal 1 km. As the fracturing pressure is increased, the gas is produced at a much faster rate. Since the total amount of gas within the defined shale region is fixed (approximately 3.8 bcf, or billion cubic feet, for the current model), the supply is exhausted more quickly at higher pressures. Note that it is not necessary to use wellbore pressures that are greater than 70 MPa. At lower wellbore pressures, the permeability of rock increases even though there is no region of tensile stress. According to Equation (2), permeability is enhanced whenever the compressive stress is decreased.

Considine (2010) reports a production curve for horizontal wells in the Marcellus Shale. The author did not, however, specify the horizontal lengths of the wells, and also noted that these numbers are on the low end of typical Marcellus Shale wells. The model presented here would agree with the reported curve at a fracturing pressure of 70 MPa (Figure 5b).

The production curve provided by Considine (2010) drops sharply after two years, but a steady amount of gas is estimated to be produced over a period spanning as large as fifty years. The author states that the total production is estimated at 3.5 bcf, approximately the same as the fixed value in this model. In this model, the natural gas production over a thirty-year period was shown to be constant, regardless of the fracturing pressure used. The model thus suggests that lower fracturing pressures (e.g., 40-50 MPa) may produce equivalent amounts of natural gas while reducing damage to the rock column.

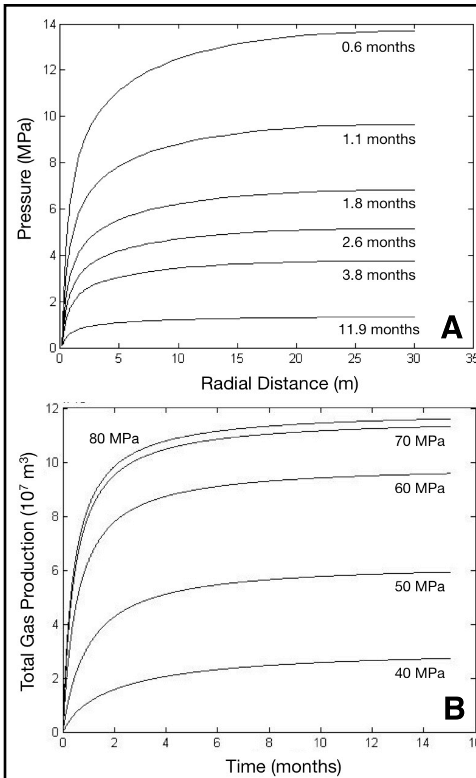

Figure 5. Numerical Results from a Simulation of Hydraulic Fracturing Stress Analysis and Gas Flow. Figure (A) shows the pressure distribution at selected values of time *t*. Note that the pressure levels to a constant value as the distance from the wellbore increases, and that this constant decreases over time. Figure (B) shows the total gas production over a fifteen month period.

Materials and Methods:

1.0-3.2 million gallons of flowback or produced water are generated at each drilling site. Laboratory experiments involved the use of these effluent waters, originating from three Marcellus Shale sites in Pennsylvania. The exact locations of these sites were not disclosed, but samples identified as FRAC-16, FRAC-17, and FRAC-18 were from Southwest Pennsylvania, Central Pennsylvania, and Northeast Pennsylvania, respectively.

Chemical Analysis of Flowback Waters:

Basic properties of each fluid-- pH, salinity, density, and viscosity-- were measured. Inductively-Coupled Plasma Optical Emission Spectroscopy (ICP-OES) was used for the presence and concentration of barium, calcium, iron, magnesium, manganese, and strontium, and Mass Spectroscopy (ICP-MS) was used to test for lead.

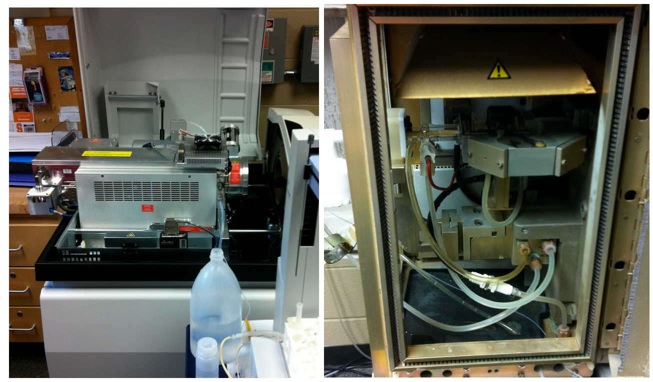

Figure 6. Inductive-Coupled Plasma Mass Spectrometry (ICP-MS, left) and Optical Emission Spectroscopy (ICP-OES, right). This instrumentation was used to find the concentration of several metal ions in effluent samples.

Black shale is the dominant lithology in the Marcellus Formation (Roen, 1984). Like other black shales, the Marcellus Formation carries naturally-occurring uranium (Vine & Tourtelot, 1970). Thus, radiation measurements for beta-emitting nuclides were conducted on the three effluent samples using a liquid scintillation counter, as per Bray (1960). 1 mL of scintillant was added to 1 mL of effluent in a glass vial, which was then loaded into the liquid scintillation counter, with a deionized water control to measure background radioactivity. Since black shales also contain large amounts of organic carbon, Total Organic Carbon Analysis for each sample.

Environmental Effluent Toxicity Analysis:

In order to determine the toxicity of hydrofracture effluent to terrestrial plant species and aquatic organisms, two assays were conducted: an 'established ecosystem' study measuring the toxicity of effluent to maturing *Brassica rapa* plants and an assay of *Hydra oligactis* (freshwater hydra) assessing the toxicity of effluent in freshwater systems.

In order to gauge the impact of a flowback water spill in an ecosystem, an 'established ecosystem' study was conducted using week-old *Brassica rapa* plants. *B. rapa* (field mustard), were grown under 24-hour fluorescent bulbs without fertilizer or additives, and watered using deionized water. After seven days, effluent was applied in concentrations of 25%, 10%, 5%, and 0% (control). Six cells, or approximately twelve *B. rapa* plants, were blocked together for one treatment; 2 mL of diluted effluent was added at the base of each plant daily. The height of each plant was measured daily before application and was standardized according to the initial height of that plant before effluent application. A two sample *t*-test was conducted to determine whether plants at 'low' concentrations of effluent (e.g. 0% and 5%) exhibited greater growth than those at 'high' concentrations of effluent (e.g. 10% and 25%).

A study of the extended environmental impacts of a flowback spill must also take into account the uptake of toxins by plant systems. Storage of heavy metals in leaf tissue allows for the possibility of biomagnification within the ecosystem. X-ray Fluorescence (XRF) was used to compare the leaf tissue concentrations of iron, selenium, strontium, and barium at various concentrations of applied effluent, as per the methodology outlined by Stephens and Calder (2004). Two leaves were randomly chosen from each *Brassica rapa* plot, and four were chosen from the control. The counts of each element per unit mass were recorded for the leaf samples, as well as for a blank XRF cell. A significance of slope test was used to determine the correlation between effluent concentration and toxin presence in leaf tissue.

Assays were also conducted using freshwater hydra. *Hydra*, a coelenterate approximately 1 cm in length, has been used as a model organism in several toxicity studies, as toxicity assays using *Hydra* are "rapid, sensitive, and precise when measuring the effect of environmental pollutants" (Pollino & Holdway, 1999). Studies note that *H. oligactis* are, in relation to other species, less sensitive to metal contaminants, yet detect ethylene bromide and other organic substances easily (Pyatt & Dodd, 1986; Herring et. al., 1998). Since the hydrofracture effluent samples are assumed to have high metal concentrations and may contain organic traces, *H. oligactis* was an ideal choice.

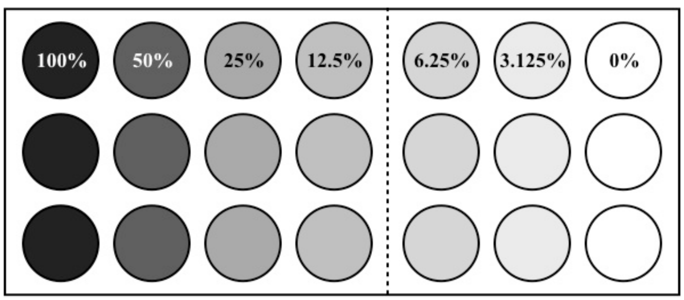

Figure 7. Two-Fold Serial Dilution-Based Assay. 4 mL of the diluted effluent was added to each well. The same assay scheme was used to conduct plant and *Hydra* assays.

Bioassays were conducted as per the methodology outlined by Trottier et. al. (1997). A two-fold serial dilution of effluent in deionized water was used, with concentrations ranging from 100% to 3.125%. As shown in Figure 7, 4 mL of diluted effluent were added to 12-well plates; individual non-budding hydra of comparable length were selected from batch cultures, and one hydra was added to each well. Hydra undergo drastic changes in morphology at greater levels of toxicity (Figure 8). Adult hydra exhibit clubbed and shortened tentacles as a first sign of intoxication, while the tulip phase leads to the death of the organism. Thus, the tulip and clubbed-tentacle stages were chosen as the endpoint for lethal and sublethal effects, respectively.

After 72 hrs, the EC_{50}, LC_{50}, and TC (threshold concentration) were calculated for each effluent sample. EC_{50} and LC_{50} values were calculated according to the trimmed Spearman-Karber method

(Hamilton, Russo, & Thurston, 1977). Lethal NOECs (no observed effect concentration) and LOECs (lowest observed effect concentration) were determined by visual observation. The threshold concentration was thus calculated (U.S. EPA, 1989):

$$TC = (NOEC \times LOEC)^{1/2} \tag{11}$$

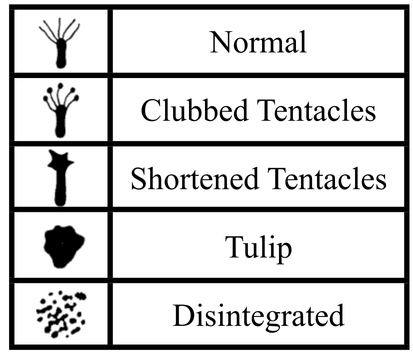

Figure 8. Morphological Changes of *Hydra* in Response to Toxins. The clubbed tentacle and tulip stages were chosen as sublethal and lethal endpoints, respectively. Figure from Blaise & Kusui (1997).

Results and Discussion:

Chemical Composition of Effluent:

Of the three hydrofracture effluents obtained, FRAC-16 and FRAC-18 appeared rosy orange in color, whereas FRAC-17 had a yellow hue. The pH, salinity, density, and viscosity of each sample are detailed in Table 1.

Table 1. Properties of Hydrofracture Effluents. While error values for pH and salinity represent the standard deviation of measurements taken, the errors for viscosity derive from the assigned uncertainty of the device used.

Property	FRAC-16	FRAC-17	FRAC-18
pH	4.01 ± 0.02	2.59 ± 0.01	3.84 ± 0.01
Salinity (ppth NaCl eq.)	235 ± 7.1	285 ± 7.1	250 ± 0.0
Density (g mL^{-1})	1.139	1.153	1.162
Viscosity (cP)	1.504 ± 0.003	1.692 ± 0.003	1.598 ± 0.003

The concentrations of barium (Ba), calcium (Ca), iron (Fe), magnesium (Mg), manganese (Mn), lead (Pb), and strontium (Sr) were determined using ICP-OES and ICP-MS (Table 2). These measurements represent perhaps the first documentation of Marcellus Shale flowback metal concentrations in literature. Note that FRAC-17's iron concentration is much smaller than that in FRAC-16 and -18. This is consistent with observations of a redder hue in the FRAC-16 and -18 samples.

Table 2. Metal Concentrations in Flowback Water Samples as Determined by ICP-OES and ICP-MS. Note the large fluctuations in iron, barium, lead, and strontium concentrations.

Metal	FRAC-16	FRAC-17	FRAC-18
Ba	394 ppm	763 ppm	15540 ppm
Ca	25980 ppm	35023 ppm	27386 ppm
Fe	99 ppm	39 ppm	129 ppm
Mg	2499 ppm	2841 ppm	2057 ppm
Mn	13 ppm	17 ppm	9 ppm
Sr	3561 ppm	5319 ppm	7127 ppm
Pb	6.86 ppb	43.23 ppb	24.86 ppb

It is apparent that these flowback waters require significant treatment before reuse. The EPA (2009) has designated 2 ppm as the maximum contaminant level (MCL) of barium in drinking water; the samples contain approximately 200, 380, and 7,700 times more barium than this standard, respectively. FRAC-17 and -18 both contain more lead than allowed by the EPA MCL 15 ppb level. Additionally, the samples each contain more than 180 times the secondary MCL (SMCL) standard for Mn and more than 40,000 times the SMCL standard for Mg.

The dissolved organic carbon (DOC) concentrations were determined by Total Organic Carbon Analysis to be 84.9 ± 4.25 ppm, 102.0 ± 5.1 ppm, and 64.5 ± 3.2 ppm, for samples FRAC-16, -17, and -18, respectively. A detailed analysis of the samples' organic content was left for future investigation.

Corporations such as ProChemTech International, Inc. have advocated reuse of effluent as hydrofracture water, rather than purification to drinking water standards. In this case, treatment standards for effluent are less stringent, yet are still required, as high metal concentrations may form precipitates and block the flow of natural gas toward the wellbore in hydraulic fracturing processes.

The beta-decay radiation measurements were as follows: 87.2 cpm (FRAC-16), 124.2 cpm (FRAC-17), 123.2 cpm (FRAC-18), and 46.1 cpm (di-H_2O, control). Since atomic nuclear decay follows the Poisson distribution, the background's standard deviation can be estimated as $\sqrt{46.1} = 6.8$ cpm. If we approximate the Poisson distribution with a normal distribution, the '*z*-scores' for the radioactivity of the three effluent samples are 6.05, 11.50, and 11.36, and the resulting *P*-values are less than 10^{-9}.

As mentioned previously, black shales are known to have naturally-occurring Uranium. The beta-emitter in the samples, then, most likely results from the Uranium-Radium series (Table 3), and is most likely Pb^{210}, which has a relatively long half-life of 22 years.

Table 3. Uranium-Radium Series (*4n + 2*) adapted from Kirby (1954). The half-lives of each isotope are given in years, months, or days.

Isotope	Decay	Half Life
U^{238}	α	4.51×10^9 Y
Th^{234}	β^-	24.10 D
Pa^{234}	β^-	1.14 M
U^{234}	α	2.67×10^5 Y
Th^{230}	α	8.00×10^4 Y
Ra^{226}	α	1.62×10^3 Y
Rn^{222}	α	3.825 D
Po^{218}	α	3.05 M
Pb^{214}	β^-	26.8 M
Bi^{214}	α	19.7 M
Pb^{210}	β^-	22 Y
Bi^{210}	β^-	4.85 D
Po^{210}	α	138.4 D
Pb^{206}	Stable	--

Toxicity Assays of Flowback Waters:

In the 'established ecosystem' experiment, a two sample *t*-test was conducted to determine whether plants at 'low' concentrations of effluent (i.e., 0% and 5%) exhibited greater growth than those at 'high' concentrations of effluent (i.e., 10% and 25%). *Brassica rapa* plants at 'low' concentrations grew an average of 1.50 times better than those at 'high' concentrations of effluent after five days of effluent application (Table 4). *P*-values confirmed that *B. rapa* plants exhibited significant stunted growth at 'high' effluent concentrations after 48 hrs of effluent application.

Table 4. 'Established Ecosystem' Data for Growth of *Brassica rapa* at 'Low' and 'High' Concentrations of Effluent. Height is stated as percentage of original height at time zero. After 48 hours of application, *Brassica rapa* at 'high' concentrations of effluent exhibit significant stunted growth.

Application Time (hrs)	Height (%): 0%, 5%	Height (%): 10%, 25%	Standard Error (SE)	Test Statistic (TS)	$P(\bar{x}_{10\%, 25\%} - \bar{x}_{0\%, 5\%} \geq 0)$
0	100 ± 0.00	100 ± 0.00	0.000	N/A	N/A
24	111.8 ± 0.02	110.9 ± 0.02	0.032	-0.278	3.91×10^{-1}
48	129.6 ± 0.03	117.2 ± 0.03	0.044	-2.806	3.20×10^{-3}
72	152.1 ± 0.05	124.1 ± 0.04	0.063	-4.406	1.73×10^{-5}
96	179.7 ± 0.06	134.9 ± 0.06	0.086	-5.216	7.84×10^{-7}
120	202.6 ± 0.07	135.4 ± 0.07	0.102	-6.583	2.78×10^{-9}

X-Ray Fluorescence (XRF) was used to measure the uptake and storage of effluent metal ions by the *Brassica rapa* plants. As shown in Table 5, concentrations of selenium, strontium, iron, and barium significantly rose with higher effluent concentration in the 0%-10% range. These results demonstrate that heavy metals found in flowback waters accumulate in leaf tissues, opening the door for biomagnification of these toxins. Future study is required to gauge the magnitude of this accumulation.

Table 5. X-Ray Fluorescence Data for Iron, Selenium, Strontium, and Barium. Significance of slope tests were conducted to find the correlation between effluent concentration and metal concentration in leaf tissues.

Metal	$\beta_{0,5,10}$	P-Value
Iron (Fe)	4,056	0.008
Selenium (Se)	181.8	0.049
Strontium (Sr)	108,200	0.000
Barium (Ba)	1,597	0.006

The *Hydra oligactis* bioassay showed that the effluent samples were toxic to hydra even at extremely low concentrations. Trimmed Spearman-Karber EC_{50} and LC_{50} values are shown in Table 6. LC_{50} and TC values for the FRAC-17 sample are slightly higher than the other two samples. This could indicate iron was an important factor in the samples' toxicity to *H. oligactis*, and that the reduced concentration of iron in FRAC-17 resulted

Table 6. EC_{50}, LC_{50}, and TC Values for *Hydra oligactis*. 95% confidence intervals using the Trimmed Spearman-Karber method are shown in parentheses.

Effluent Sample	EC_{50} (%) 72 hrs.	LC_{50} (%) 72 hrs.	TC (%) 72 hrs.
FRAC-16	**3.72**	**11.14** (7.64, 16.24)	8.84
FRAC-17	**4.42** (1.99, 9.84)	**28.06** (19.24, 40.92)	17.68
FRAC-18	**3.72**	**14.03** (7.30, 26.97)	4.42

in a smaller mortality rate. Regardless, TC values were very low for all samples, suggesting that effluent could prove extremely hazardous to freshwater ecosystems.

Conclusions and Future Work:

This study provides a comprehensive examination of the various aspects of hydraulic fracturing in Upstate New York. A mathematical model was developed to determine the effect of process parameters (e.g., fracturing fluid pressure and wellbore radius) on gas production. It was shown that a well in Upstate New York extending 1 km horizontally produces approximately 3-4 billion cubic feet (bcf) of natural gas, an amount comparable with publicly available data. The model demonstrated that lower fracturing pressures (40-50 MPa) may produce equivalent amounts of natural gas over a long period of time, while mitigating structural damage to the rock column and thereby lessening the mobility of toxins upward to shallow water aquifers.

An extensive analysis of Marcellus Shale flowback included both chemical composition studies and an assessment of environmental toxicity. The samples were shown to have high concentrations of barium, strontium, and lead and exhibit beta decay, most likely attributed to Pb^{210} isotopes. These measurements are the first documentation of metal concentrations and radioactivity in hydraulic fracturing effluent. An ‘established ecosystem’ experiment showed that heavy metals may accumulate in *B. rapa* leaf tissues. Finally, effluent was found to be extremely toxic to freshwater organisms such as *Hydra oligactis*; EC_{50} and LC_{50} values were as low as 3.7% and 11.1%, respectively.

The study can be extended in several ways. The model can be modified to account for a non-circular boundary, anisotropic permeability, and a more detailed simulation of fracture propagation. The link between hydraulic fracturing and earthquake-occurrence also requires investigation. Recent studies have noted that micro-earthquakes caused by fracturing may further increase rock permeability and gas flow to the wellbore (M. D. Zoback, personal communication, Aug. 16, 2011). A more complex model may simulate microseismic events’ effect on stress distributions and rock structure permeability.

Future work is needed for developing cost-effective methods that remove heavy metals and radioactive substances. Although TOC Analysis determined the concentration of dissolved organic carbon in each sample, the constituents of this organic portion have yet to be determined; organic extraction and other techniques may determine the presence and concentration of hydrocarbons.

References

Ameen, M. S. (1995). Fractography: Fracture Topography as a Tool in Fracture Mechanics and Stress Analysis. Geological Society Special Publication, 92, 187-196.

Blaise, C. & T. Kusui (1997). Acute Toxicity Assessment of Industrial Effluents with a Microplate-Based *Hydra attenuata* Assay. Environmental Toxicology and Water Quality, 12, 53-60.

Bray, G. A. (1960). A Simple Efficient Liquid Scintillator for Counting Aqueous Solutions in a Liquid Scintillation Counter. Analytical Biochemistry, 1, 279-285.

Considine, T. J. (2010). The Economic Impacts of the Marcellus Shale: Implications for New York, Pennsylvania, and West Virginia (prepared for The American Petroleum Institute). Laramie, Wyoming: Natural Resource Economics, Inc.

Curtis, J. B. (2011). Potential Gas Committee Reports Substantial Increase in Magnitude of U.S. Natural Gas Resource Base. Golden, Colorado: Colorado School of Mines Potential Gas Agency.

Farlow, S. J. (1993). Partial Differential Equations for Scientists and Engineers. NY: Dover Publications.

Hamilton, M. A., R. C. Russo, & R. V. Thurston (1977). Trimmed Spearman-Karber Method for Estimating Median Lethal Concentration in Toxicity Bioassays. Environmental Science and Technology, 11, 714-719.

Harper, J. (2008). The Marcellus Shale: An Old "New" Gas Reservoir in Pennsylvania. Published by the Bureau of Topographic and Geologic Survey, Pennsylvania Department of Conservation and Natural Resources. Pennsylvania Geology, 38, 2-12.

Herring, C. O. et. al. (1988). Dose-Response Studies Using Ethylene Dibromide (EDB) in *Hydra oligactis*. Bulletin of Environmental Contamination and Toxicology, 40, 35-40.

Hill, D. G. & T. E. Lombardi (2002). Fractured Gas Shale Potential in New York (New York State Energy Research and Development Authority). Arvada, Colorado: TICORA Geosciences, Inc.

Karacan, C. O., G. S. Esterhuizen, S. J. Schatzel, & W. P. Diamond (2006). Reservoir Simulation-Based Modeling for Characterizing Longwall Methane Emissions and Gob Gas Venthole Production. International Journal of Coal Geology, 71, 225-245.

Karlsson et. al. (1992). Method and Apparatus for Horizontal Drilling. *U.S. Patent No. 5,148,875*. Washington, D.C.: U.S. Patent and Trademark Office.

Kirby, H. W. (1954). Decay and Growth Tables for the Naturally Occurring Radioactive Series. Analytical Chemistry, 26, 1063-1071.

Osborn, S. G., A. Vengosh, N. R. Warner, & R. B. Jackson. (2011). Methane Contamination of Drinking Water Accompanying Gas-Well Drilling and Hydraulic Fracturing. Proceedings of the National Academy of Sciences of the United States of America, 108, 8172-8176.

Pollino, C. A. & D. A. Holdway (1999). Potential of Two Hydra Species as Standard Toxicity Test Animals. Ecotoxicology and Environmental Safety, 43, 309-316.

Pyatt, F. B. & N. M. Dodd (1986). Some Effects of Metal Ions on the Freshwater Organisms, *Hydra oligactis* and *Chlorohydra viridissima*. Indian Journal of Experimental Biology, 24, 169-173.

Roen, J. B. (1984). Geology of the Devonian Black Shales of Appalachian Basin. Organic Geochemistry, 5, 241-254.

Rogner, H. H. (1997). An Assessment of World Hydrocarbon Resources. Annual Review of Energy and the Environment, 22, 217-262.

Smith, G. D. (1986). Numerical Solutions of Partial Differential Equations: Finite Difference Methods. New York: Oxford University Press.

Soeder, D. J. (1986). Porosity and Permeability of Eastern Devonian Gas Shale. SPE Formation Evaluation, 3 (1), 116-124.

Stephens, W. E. & A. Calder (2004). Analysis of Non-Organic Elements in Plant Foliage Using Polarised X-ray Fluorescence Spectroscopy. Analytica Chimica Acta, 527, 89-96.

Trottier, S., C. Blaise, T. Kusui, & E. M. Johnson (1997). Acute Toxicity Assessment of Aqueous Samples Using a Microplate-Based *Hydra attenuata* Assay. Environmental Toxicology and Water Quality, 12, 265-271.

U. S. Environmental Protection Agency (2009). National Primary Drinking Water Regulations. Washington, D. C.: Government Printing Office.

U.S. Environmental Protection Agency (1989). Short-Term Methods for Estimating the Chronic Toxicity of Effluents and Receiving Wastes to Freshwater Organisms. EPA/600/4-89/001, Office of Research and Development, Cincinnati, OH, 248 p.

Vine, J. D. & E. B. Tourtelot (1970). Geochemistry of Black Shale Deposits: A Summary Report. Economic Geology, 65, 253-283.

Volz, C. D. et al. (2011). *Contaminant Characterization of Effluent from Pennsylvania Brine Treatment Inc., Josephine Facility Being Released into Blacklick Creek, Indiana County, Pennsylvania*. Center for Health Environments and Communities (CHEC).